

Determination of double- K fracture parameters of concrete using split-tension cube test

Shailendra Kumar^{1,2*} and S.R. Pandey²

¹Department of Civil Engineering, Institute of Technology, Guru Ghasidas Vishwavidyalaya
(A Central University), Bilaspur - 495009, Chhattisgarh, India

²Department of Civil Engineering, National Institute of Technology, Jamshedpur-831014, Jharkhand, India

(Received August 6, 2010, Revised January 26, 2011, Accepted April 6, 2011)

Abstract. This paper presents development of double- K fracture model for the split-tension cube specimen for determining the unstable fracture toughness and initial cracking toughness of concrete. There are some advantages of using of split-tension cube test like compactness and lightness over the existing specimen geometries in practice such as three-point bend test, wedge splitting test and compact tension specimen. The cohesive toughness of the material is determined using weight function having four terms for the split-tension cube specimen. Some empirical relations are also suggested for determining geometrical factors in order to calculate stress intensity factor and crack mouth opening displacement for the same specimen. The results of double- K fracture parameters of split-tension cube specimen are compared with those obtained for compact tension specimen. Finally, the influence of the width of the load-distribution of split-tension cube specimen on the double- K fracture parameters for laboratory size specimens is investigated. The input data required for determining double- K fracture parameters for both the specimen geometries are obtained using well known version of the Fictitious Crack Model.

Keywords: split-tension cube test; compact tension test; concrete fracture; double- K fracture parameters; weight function; cohesive stress; size-effect.

1. Introduction

Fracture behavior of quassibrittle material like concrete is different than that of brittle and elastic-plastic materials. While the nonlinear behavior in elastic-plastic material is mainly due to existence of plasticity near a crack-tip, the nonlinear fracture behavior in concrete is exhibited mainly due to existence of large and variable size of fracture process zone (FPZ) ahead of a crack under external loading. The development of FPZ is associated with three different stages of crack propagation in concrete: crack initiation, stable crack propagation and unstable fracture (Xu and Reinhardt 1999a). This is why the direct application of linear elastic fracture mechanics (LEFM) fails to predict a constant value of fracture toughness of the material for different geometrical properties and sizes of test specimens. The evolution of FPZ can be suitably accounted for in the nonlinear fracture models based on numerical approach such as cohesive crack model (CCM) or fictitious crack model (FCM) (Hillerborg *et al.* 1976, Petersson 1981, Carpinteri 1989, Planas and Elices 1991) and crack band model (CBM) (Bažant and Oh 1983) and the modified form of LEFM concept such as two parameter fracture model (TPFM) (Jenq and Shah 1985), size effect model (SEM) (Bažant *et al.* 1986), effective

* Corresponding author, Ph. D., E-mail: shailendrakmr@yahoo.co.in

crack model (ECM) (Nallathambi and Karihaloo 1986), K_R -curve method based on cohesive force distribution (Xu and Reinhardt 1998, 1999a), double- K fracture model (DKFM) (Xu and Reinhardt 1999(a)-(b)) and double- G fracture model (DGM) (Xu and Zhang 2008). The FCM and CBM are based on finite element or boundary element methods which take into account of fracture process zone by means of constitutive relations showing strain softening and strain localization during the crack propagation. The other fracture models using modified form of LEFM approach account for the effect of nonlinearity in the material behavior due to existence of process zone and have a practical advantage that the fracture properties of concrete can be determined with relatively less computational effort as compared to those based on numerical approach. The fracture models based on modified LEFM concept such as DKFM, DGM and the K_R -curve method associated with cohesive force distribution can capture all the three important stages of crack propagation in concrete whereas the fracture models under the same category such as TPFM, SEM and ECM predict the fracture loads at critical condition only. While DKFM is based on stress intensity factor (SIF) approach, DGM is based on the concept of energy release rate and therefore ductility property is also associated with it. However, the characteristic parameters of DKFM, i.e. initial cracking toughness K_{IC}^{ini} and unstable fracture toughness K_{IC}^{un} can be evaluated with relatively less effort particularly when the weight function method recently proposed by the authors (Kumar and Barai 2008a, 2009a, 2010) is used. The parameter K_{IC}^{ini} is directly calculated by the initial cracking load and initial notch length using LEFM formula whereas the other parameter K_{IC}^{un} can be obtained by peak load and corresponding effective crack length using the same LEFM formula. Xu and Reinhardt (1999(b)-(c)) developed analytical method for three-point bending test (TPBT) and compact tension (CT) specimen or wedge splitting test (WST) to determine the values of double- K fracture parameters. Later, a *simplified approach* (Xu and Reinhardt 2000) was proposed using two empirical formulae to obtain the double- K fracture parameters for TPBT configuration. Kumar and Barai (2008a) presented a comparative study on determination of double- K fracture parameters using existing analytical method, simplified approach and the weight function approach for TPBT and CT test specimen geometries.

Stable fracture testing of quasibrittle material like concrete using indirect method can be carried out with the specimen of various geometrical shapes such as three-point bending test (TPBT), four-point bending test (FPBT), compact tension (CT) test and wedge splitting test (WST). The three-point bending geometry (RILEM Technical Committee 50-FMC 1985) is a common specimen used to determine the fracture parameters applying the different fracture models because of an advantage that the testing can be performed with the standard testing machines and it is easier to perform the stable bending test on pre-cracked beams. However, for large size structures, the self-weight of the beam possibly negates the use of the specimen for fracture testing due to not only handling problems of testing specimens but also requiring special care in fracture analysis. In addition, it is not practically possible to use as a drilled specimen from the construction sites or existing structures. Alternatively, CT test (ASTM standard E-399 2006) and WST (Tschegg 1986, Wittmann *et al.* 1988, Brühwiler and Wittmann 1990) have been used by many researchers in the past to determine the fracture parameters of concrete. The CT specimen also suffers from some drawbacks such as there are no flexibilities in specimen shapes such that drilling of specimen from existing structures is difficult, there may be inconvenient with testing arrangement in directly applying the load on the specimen and the testing can be carried out only crack opening displacement (COD) controlled test setup. The wedge-splitting test is a special form of the so-called compact tension test, in which a small specimen with a groove and notch is split in two halves while monitoring the load

and crack mouth opening displacement (CMOD). There are several advantages of using WST specimen for stable fracture testing of concrete over TPBT and CT specimen like: specimen compactness, providing relatively larger ligament area to concrete volume ratio, not being affected by self-weight of the specimen, being cubical or cylindrical in shapes and suitable for fracture testing from existing structures using drilled concrete cores and suitable for displacement of the wedges or in closed-loop COD controlled testing. Tensile properties of concrete are most frequently determined using cylindrical and cubical split-tension specimens nowadays called Brazilian split test (Carneiro and Barcellos 1949, Nilsson 1961) because of many advantages such as simplicity of preparation and performance of the test, same testing specimens and equipment as the compression strength test and relatively narrow depression of test results (Kadleček *et al.* 2002). In split-tension test, a cylindrical/cubical specimen is placed between the platens of test machine and the compressive load is applied along its horizontal axis until failure which is the split of the specimen in two halves across the plane of the loading due to development of lateral tensile stress distribution. Multiple cracking and crushing of the material at the point of loading is prevented by distributing the load using variable width of two bearing strips. The developed maximum tensile stress across the plane of the loading approaches the theoretical limit for a concentrated load when the load bearing-strips are very narrow (Rocco *et al.* 1999). In addition to perform uniaxial tensile strength, split-tension tests have successfully been used for determining fracture parameters of concrete in the past (Karihaloo 1986, Bažant *et al.* 1991, Tang *et al.* 1996, Yang *et al.* 1997, Rocco *et al.* 1999, Ince and Arici 2004, Ince 2010) because of several advantages over the testing of other specimens like TPBT, CT and WST specimens. These advantages are: compactness and lightness of specimen, easy in casting of specimen that can be also used in strength tests, specimen can be easily prepared by drilling of concrete cores from existing structures, simplicity in performing the test and therefore avoiding the need of special loading and testing arrangement, insignificant influence of self weight of the specimen in testing and analysis. Apart from the common advantages with using split-tension cylinder or cube specimen, the cube specimen can be modeled relatively easily than that of cylinder specimen because of straight boundaries are available in cube specimen and hence simple finite element program can be easily employed in this case.

The results of fracture toughness of plain concrete obtained from compression splitting tests (Karihaloo 1986) showed that fracture toughness does not vary with the shape and size of the specimens provided that width of the compression platen and the depth of the pre-crack are within well defined limits ensuring failure of specimens by axial splitting. Bažant *et al.* (1991) carried out experimental and theoretical studies on split-tension cylinder tests which confirmed the existence of size effect. The analysis of test results further showed that up to a certain critical diameter, the curve of nominal strength versus diameter approximately agrees well with the law proposed by Bažant's for the size effect caused by energy release due to fracture growth. Beyond that diameter the curve of nominal strength versus diameter approaches a horizontal asymptote, which signifies disappearance of size effect. The slope of this curve may remain either negative or reverse to positive on approach to the asymptotic strength. Experimental test results carried out by Yang *et al.* (1997) confirmed that the peak-load method can be successfully applied to splitting tension cylinder tests to determine the fracture parameters of two parameter fracture model. Tang *et al.* (1996) proposed a new version of size effect law for determining the fracture parameters of size effect model using specimen of only one shape and one size but with different notch lengths. In the study, it was concluded that holed split-tension cylinder is suitable specimen shape for determining the fracture properties. Rocco *et al.* (1999) applied cohesive crack model to derive the size-effect curves for the splitting tensile strength

of concrete on cylindrical and prismatic square section specimens. Two important variables such as the load-bearing strip and the geometry of the specimen were studied. The reported results confirmed that splitting strength decreases with the specimen size, tending towards an asymptotic solution for large size specimens. It was concluded that the dependence of the splitting tensile strength on the specimen size and on the width of the bearing strip should be taken into account when using the Brazilian test. On the basis of experimental and statistical investigations for size effect of bearing strength of concrete cubes, Ince and Arici (2002) concluded that the observed test results were in good agreement with Bažant's size effect law. Ince (2010) calculated the fracture parameters of concrete using two-parameter fracture model and size effect model and carried out a comparative study among the splitting-cube specimen, splitting-cylindrical specimen and three-point bending test with regard to the obtained results. In order to determine the fracture parameters of cube specimen, the linear elastic fracture mechanics formulas namely the stress intensity factor, the crack mouth opening displacement and the crack opening displacement profile were determined for different load-distributed widths using the finite element method. In the recent past, many research and studies using experimental test results and numerical analyses on TPBT, CT and WST specimens (Kumar 2010) have been carried out to show the behavior of fracture parameters of double- K fracture model. As far as authors' knowledge is concerned, no such study has been carried out in the existing literature considering split-tension cube specimen. Therefore, development of double- K fracture model using split-tension cube test will open up a new direction for this model for characterizing the material fracture parameters.

The main objective of the paper is to develop computational procedure of double- K fracture model using *weight function method* for the split-tension cube specimen of concrete. Some empirical relations are also derived for determining geometrical factors in order to calculate stress intensity factor and crack mouth opening displacement for split-tension cube specimen. The results of double- K fracture parameters of split-tension cube specimen are compared with those obtained for compact tension specimen. Towards the end, the influence of the width of the load-distribution of split-tension cube specimen on the double- K fracture parameters for laboratory size specimens is studied. The input data required for determining for both the specimen geometries are obtained using well known version of the FCM.

2. Dimensions of test specimens

Determination of the double- K fracture parameters for STC specimen is proposed in the present work and the results are compared with those obtained using CT specimen. For this study, the standard test geometries, dimensions and loading conditions for STC and CT specimens are considered as shown in Fig. 1.

The symbols in Fig. 1(a): a_o , D , h and t are half of the initial notch-length, characteristic dimension as specimen size ($D = h/2$), height or total depth and half of the width of distributed load respectively for STC geometry. The dimensions and configuration of standard CT specimen according to the ASTM standard E-399 (2006) are shown in Fig. 1(b) for which a_o is the initial notch-length, D is the characteristic dimension as specimen size, $D_1 = 1.25D$, $H = 0.6D$, $H_1 = 0.275D$ and $B = 0.5D$. The B is the specimen thickness for both the specimen geometries.

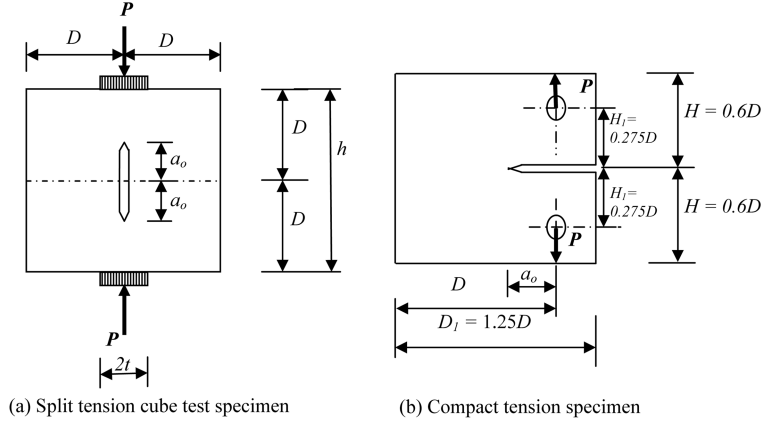


Fig. 1 Dimensions and loading schemes for STC and CT test specimens

3. Determination of double-K fracture parameters for STC specimen

3.1 Assumptions

Linear asymptotic superposition assumption is considered to introduce LEM for calculating the double-K fracture parameters. The hypotheses of the assumption are given below:

1. the nonlinear characteristic of the load-crack mouth opening displacement (P-CMOD) curve is caused by fictitious crack extension in front of a stress-free crack; and
2. an effective crack consists of an equivalent-elastic stress-free crack and equivalent-elastic fictitious crack extension.

A detailed explanation of the hypotheses may be seen elsewhere (Xu and Reinhardt 1999b).

3.2 Effective crack extension

For the applied load (Fig. 1) on the STC specimen, the CMOD_c is measured across the crack faces at the centre of specimen. The P-CMOD for this test geometry should be known *a priori* for determining the value of effective crack extension during the crack propagation. Using linear asymptotic superposition assumption, the equivalent-elastic crack length a_c corresponding to maximum load P_u is solved using the following formulae (Ince 2010).

The compliance C is expressed as

$$CMOD = \frac{\pi D \sigma_N}{E} \alpha V(\alpha, \beta) \quad (1)$$

$$V(\alpha, \beta) = B_0(\beta) + B_1(\beta)\alpha + B_2(\beta)\alpha^2 + B_3(\beta)\alpha^3 \quad (2)$$

In which $\alpha = a/D$, β is the relative load-distributed width and taken as $\beta = 2t/h = t/D$, $V(\alpha, \beta)$ is dimensionless function, coefficients B_i ($i = 0$ to 3) are the function of β and given in Table 1. Eq. (2) is valid for $0.1 \leq \alpha \leq 0.6$ within 0.1% accuracy for $0 \leq \beta \leq 0.2$. Since the values of coefficients B_i (Table 1) are given (Ince 2010) at discrete interval, these coefficients can be derived in the form of simple polynomial empirical equations using least square technique as given below.

Table 1 The values of coefficients A_i and B_i for split-tension cube specimen (Ince 2010)

Coefficient	$\beta = t/D$					
	0.0	0.067	0.1	0.133	0.167	0.2
A_0	0.986	0.981	0.974	0.964	0.951	0.935
A_1	0.071	0.039	0.007	-0.037	-0.079	-0.118
A_2	0.979	1.097	1.218	1.371	1.514	1.638
A_3	0.252	0.041	-0.188	-0.479	-0.778	-1.068
B_0	1.254	1.245	1.235	1.221	1.202	1.180
B_1	0.116	0.101	0.085	0.062	0.040	0.014
B_2	1.125	1.173	1.225	1.298	1.363	1.436
B_3	1.156	1.053	0.932	0.771	0.598	0.407

$$\begin{aligned}
B_0 &= 14.56\beta^4 - 6.469\beta^3 - 0.885\beta^2 - 0.050\beta + 1.254 \\
B_1 &= 7.084\beta^3 - 4.039\beta^2 + 0.015\beta + 0.116 \\
B_2 &= -31.22\beta^3 + 14.62\beta^2 - 0.126\beta + 1.124 \\
B_3 &= -12383\beta^5 + 6563\beta^4 - 1190\beta^3 + 68.42\beta^2 - 2.501\beta + 1.156
\end{aligned} \tag{3}$$

The determination coefficient R^2 is between 0.9999 and 1.00 for each regression analysis of Eq. (3) which can be conveniently used in computer program for any value of β in the range of $0 \leq \beta \leq 0.2$ and hence the proposed Eq. (3) is used in the present study.

Also, the nominal stress for STC test specimen in Eq. (1) can be written using the following formula (Timoshenko and Goodier 1970).

$$\sigma_N = \frac{2P}{\pi Bh} \tag{4}$$

At critical condition that is at maximum load P_u the half of crack length a becomes equal to a_c and σ_N to σ_{Nu} in which σ_{Nu} is the maximum nominal stress. Karihaloo and Nallathambi (1991) concluded that almost the same value of E might be obtained from P-CMOD curve, load-deflection curve and compressive cylinder test. Hence, in case initial compliance is not known the value of E determined using compressive cylinder tests may be used to obtain the critical crack length of the specimen.

3.3 Calculation of double-K fracture parameters

A linearly varying cohesive stress distribution is assumed in the fictitious crack zone, which gives rise to cohesion toughness as a part of total toughness of the cracked body. Superposition method is used in order to calculate the SIF at the tip of effective crack length K_I . According to this method, total stress intensity factor K_I is taken as the summation of stress intensity factor caused due to external load K_I^P and stress intensity factor contributed by cohesive stress K_I^C as shown in Fig. 2. The value of K_I is expressed in the following expression

$$K_I = K_I^P + K_I^C \tag{5}$$

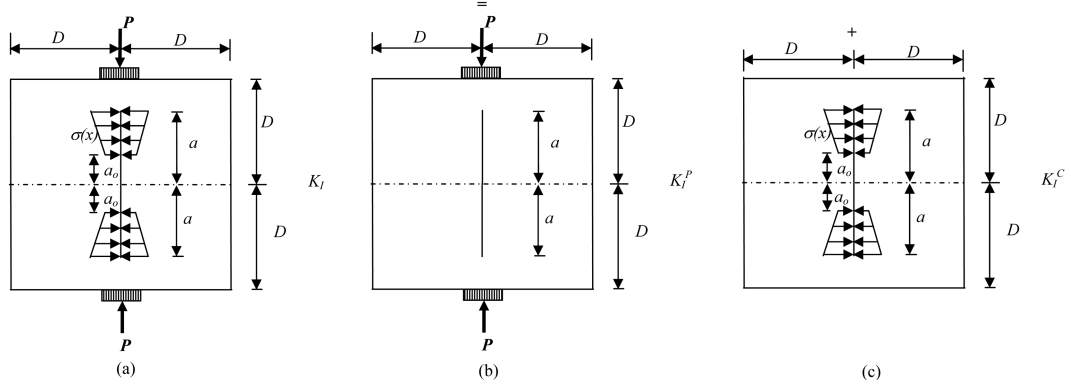


Fig. 2 Calculation of SIF using superposition method

After determining the critical effective crack extension at unstable condition of loading, both the characteristic fracture parameters K_{IC}^{ini} and K_{IC}^{un} are determined using LFM formulae (Ince 2010) and the SIF is expressed as

$$K_I = \sigma_N \sqrt{D} k(\alpha, \beta) \quad (6)$$

$$k(\alpha, \beta) = A_0(\beta) + A_1(\beta)\alpha + A_2(\beta)\alpha^2 + A_3(\beta)\alpha^3 \quad (7)$$

where $k(\alpha, \beta)$ is a geometric factor and coefficients A_i ($i=0$ to 3) are the function of β and summarized in Table 1. Eq. (7) has better than 0.3 percent accuracy for $0.1 \leq \alpha \leq 0.6$ for $0 \leq \beta \leq 0.2$.

As observed from Table 1, the values of coefficients A_i are given at discrete interval which can be empirically derived in the form of simple polynomial empirical equations using least square technique as given below.

$$\begin{aligned} A_0 &= -261.2\beta^5 + 133.7\beta^4 - 24.16\beta^3 + 0.460\beta^2 - 0.031\beta + 0.986 \\ A_1 &= -5091\beta^5 + 2821\beta^4 - 539.9\beta^3 + 37.77\beta^2 - 1.331\beta + 0.071 \\ A_2 &= 13179\beta^5 - 7222\beta^4 + 1329\beta^3 - 81.72\beta^2 + 3.177\beta + 0.979 \\ A_3 &= -17443\beta^5 + 9447\beta^4 - 1697\beta^3 + 87.63\beta^2 - 3.889\beta + 0.252 \end{aligned} \quad (8)$$

The determination coefficient R^2 is 1.00 for each regression analysis of Eq. (6) for $0 \leq \beta \leq 0.2$. Proposed Eq. (8) is used in the developed computer code for present study. If the crack initiation load P_{ini} is known from experiment, the initiation toughness K_{IC}^{ini} is calculated using Eq. (6) in which P is equal to P_{ini} and a is equal to a_0 . Alternatively, it can be determined applying the following relation.

$$K_{IC}^{ini} = K_{IC}^{un} - K_{IC}^C \quad (9)$$

Eq. (9) is known as inverse method for determining the initiation toughness.

4. Determination of SIF due to cohesive stress K_I^c

4.1 Cohesive stress distribution

The cohesive stress acting in the fracture process zone on STC test specimen is idealized as series of pair normal forces subjected symmetrically to central cracked specimen of finite width as shown in Fig. 3. The linearly varying distribution of cohesive stress is also shown in Fig. 4.

The SIF due to cohesive stress distribution as shown in Fig. 4 becomes to cohesive toughness K_{IC}^c of the material at the critical loading condition with negative value because of closing stress in fictitious fracture zone. However, the absolute value of K_{IC}^c is taken as a contribution of the total fracture toughness (Xu and Reinhardt 1999b) at the critical condition. At this loading condition, the crack-tip opening displacement (CTOD) is termed as critical crack-tip opening displacement ($CTOD_c$). In Fig. 4 $\sigma_s(CTOD_c)$ is cohesive stress at the tip of initial notch when $CTOD$ is equal to $CTOD_c$ and then $\sigma(x)$ can be expressed as

$$\sigma(x) = \sigma_s(CTOD_c) + \frac{x-a_0}{a-a_0} [f_i - \sigma_s(CTOD_c)] \text{ for } 0 \leq CTOD \leq CTOD_c \quad (10)$$

The value of $\sigma_s(CTOD_c)$ is calculated using softening functions of concrete. In the present work, the nonlinear softening function (Reinhardt *et al.* 1986) is used for the computation which can be expressed as

$$\sigma(w) = f_i \left\{ \left[1 + \left(\frac{c_1 w}{w_c} \right)^3 \right] \exp\left(\frac{-c_2 w}{w_c} \right) - \frac{w}{w_c} (1 + c_1^3) \exp(-c_2) \right\} \quad (11)$$

The value of total fracture energy of concrete G_F is expressed as

$$G_F = w_c f_i \left\{ \frac{1}{c_2} \left[1 + 6 \left(\frac{c_1}{c_2} \right)^3 \right] - \left[1 + c_1^3 \left(1 + \frac{3}{c_2} + \frac{6}{c_2^2} + \frac{6}{c_2^3} \right) \right] \frac{\exp(-c_2)}{c_2} - \left(\frac{1 + c_1^3}{2} \right) \exp(-c_2) \right\} \quad (12)$$

In which, $\sigma(w)$ is the cohesive stress at crack opening displacement w at the crack-tip and c_1 and c_2 are the material constants. Also, $w = w_c$ for $f_i = 0$, i.e., w_c is the maximum crack opening displacement at the crack-tip at which the cohesive stress becomes to be zero. The value of w_c is computed using

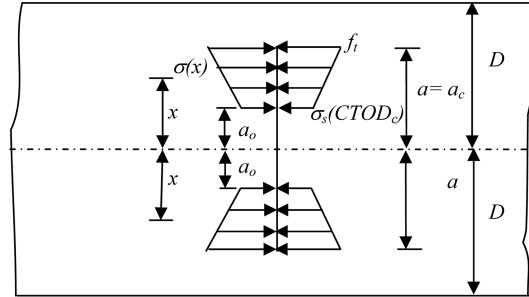
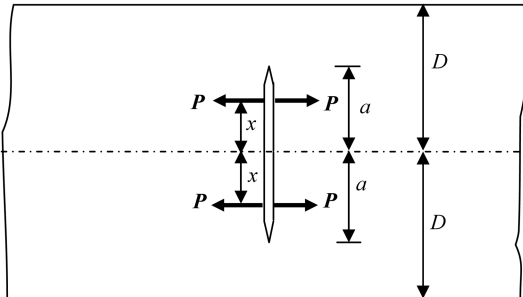


Fig. 3 Central cracked specimen of finite width subjected to pair of normal forces

Fig. 4 Distribution of cohesive stress in the fictitious crack zone at critical load

Eq. (12) for a given set of values c_1 , c_2 and G_{F_c} . For normal concrete the value of c_1 and c_2 is taken as 3 and 7 respectively.

4.2 Determination of $CTOD_c$

The value of crack mouth opening displacement at critical loading condition is termed as critical crack mouth opening displacement $CMOD_c$ and the crack opening displacement within the crack length $COD(x)$ is computed for the known value of $CMOD_c$ using the following expression (Ince 2010).

$$COD(x) = CMOD_c \{ (1-x/a)^2 + (2.067 - 0.425a/D)[x/a - (x/a)^2] \}^{1/2} \quad (13)$$

The value of x is taken as a_o and a as a_c for evaluation of $CTOD_c$ using Eq. (13).

4.3 Calculation of SIF K_I^C using weight function approach

Weight function approach initially proposed by Bueckner (1970) and Rice (1972) provides a powerful technique to calculate SIFs for a cracked body subjected to arbitrary stress fields. According to this method, the mode-I SIF for distribution of stress $\sigma(x)$ along the crack line x in the uncracked body is given by following expression.

$$K_I = \int_0^a \sigma(x).m(x,a)dx \quad (14)$$

In which, the term $m(x, a)$ is known as weight function, a is the crack length and dx is the infinitesimal length along the crack surface. The authors (Kumar and Barai 2008a, 2009a, 2010) introduced *weight function method* for determining the double-K fracture parameters of TPBT and CT specimens based on universal form of weight function (Glinka and Shen 1991). This method provides a closed form solution for determining K_{IC}^C for a trapezoidal cohesive stress distribution in the FPZ and thus avoiding the need of specialized numerical technique because of singularity problem at integral boundary. The four term universal form of weight function (Glinka and Shen 1991) is written as

$$m(x,a) = \frac{2}{\sqrt{2\pi(a-x)}} [1 + M_1(1-x/a)^{1/2} + M_2(1-x/a) + M_3(1-x/a)^{3/2}] \quad (15)$$

For central through cracked specimen of finite width subjected to pairs of normal forces symmetrically (Fig. 3), the weight function as given by Tada *et al.* (2000) is expressed as

$$G(x,a) = \frac{2}{\sqrt{2D}} \left\{ 1 + 0.297 \sqrt{1 - \left(\frac{x}{a}\right)^2} \left[1 - \cos\left(\frac{\pi a}{2D}\right) \right] \right\} F\left(\frac{a}{D}, \frac{x}{a}\right)$$

$$F\left(\frac{a}{D}, \frac{x}{a}\right) = \sqrt{\tan\left(\frac{\pi a}{2D}\right)} \left[1 - \left(\frac{\cos\frac{\pi a}{2D}}{\cos\frac{\pi x}{2D}} \right)^2 \right]^{-1/2} \quad (16)$$

Eq. (16) can equivalently be expressed in terms of universal weight function $m(x, a)$ of Eq. (15)

with the following weight function parameters M_1 , M_2 and M_3 (Wu *et al.* 2003).

$$m_1 = 0.06987 + 0.40117\left(\frac{a}{D}\right) - 5.5407\left(\frac{a}{D}\right)^2 + 50.0886\left(\frac{a}{D}\right)^3$$

$$M_1 = m_1 - 200.699\left(\frac{a}{D}\right)^4 + 395.22\left(\frac{a}{D}\right)^5 - 377.939\left(\frac{a}{D}\right)^6 + 140.218\left(\frac{a}{D}\right)^7 \quad (17)$$

$$m_2 = -0.09049 - 2.14886\left(\frac{a}{D}\right) + 22.5325\left(\frac{a}{D}\right)^2 - 89.6553\left(\frac{a}{D}\right)^3$$

$$M_2 = m_2 + 210.599\left(\frac{a}{D}\right)^4 - 239.445\left(\frac{a}{D}\right)^5 + 111.128\left(\frac{a}{D}\right)^6 \quad (18)$$

$$m_3 = 0.427216 + 2.56001\left(\frac{a}{D}\right) - 29.6349\left(\frac{a}{D}\right)^2 + 138.4\left(\frac{a}{D}\right)^3$$

$$M_3 = m_3 - 347.255\left(\frac{a}{D}\right)^4 + 457.128\left(\frac{a}{D}\right)^5 - 295.882\left(\frac{a}{D}\right)^6 + 68.1575\left(\frac{a}{D}\right)^7 \quad (19)$$

Eqs. (17)-(19) are valid for $0 < a/D < 0.9$. Once the weight function parameters are determined, Eq. (15) is used to calculate the SIF at critical condition due to trapezoidal cohesive stress distribution as shown in Fig. 4. The value of $\sigma(x)$ in Eq. (14) is replaced by Eq. (10), hence the closed form expression of K_{IC}^C can be obtained according to the following form.

$$K_{IC}^C = \frac{2}{\sqrt{2\pi a}} \left\{ A_1 a \left[2s^{1/2} + M_1 s + \frac{2}{3} M_2 s^{3/2} + \frac{M_3}{2} s^2 + \frac{2}{5} M_4 s^{5/2} \right] + \right.$$

$$A_2 a^2 \left[\frac{4}{3} s^{3/2} + \frac{M_1}{2} s^2 + \frac{4}{15} M_2 s^{5/2} + \frac{4}{35} M_4 s^{7/2} + \frac{M_3}{6} \{ 1 - (a_o/a)^3 - 3s a_o/a \} \right] \quad (20)$$

where, $A_1 = \sigma_s(CTOD_c)$, $A_2 = \frac{f_t - \sigma_s(CTOD_c)}{a - a_o}$ and $s = (1 - a_o/a)$, also $a = a_c$ at $P = P_u$. After determining the value of K_{IC}^C using Eq. (20), initiation toughness can be evaluated using Eq. (9).

5. Fictitious crack model and material properties for double-K fracture model

The cohesive crack model (Hillerborg *et al.* 1976, Petersson 1981, Carpinteri 1989, Planas and Elices 1991, Kumar and Barai 2008b-2009b) is developed for STC and CT specimens to determine the input data such as P_u and $CMOD_c$ for STC or COD_c for CT specimens being the primary requirements to determine the double-K fracture parameters. Three material properties such as modulus of elasticity E , uniaxial tensile strength f_b and fracture energy G_F are required to model FCM. In this method, the governing equation of COD along the potential fracture line is written. The influence coefficients of the COD equation are determined using linear elastic finite element method. Four noded isoparametric plane elements are used in finite element calculation. The COD vector is partitioned according to the enhanced algorithm introduced by Planas and Elices (1991). Finally, the system of nonlinear simultaneous equation is developed and solved using Newton-Raphson method. For standard STC and CT specimens with $B = 100$ mm having size range

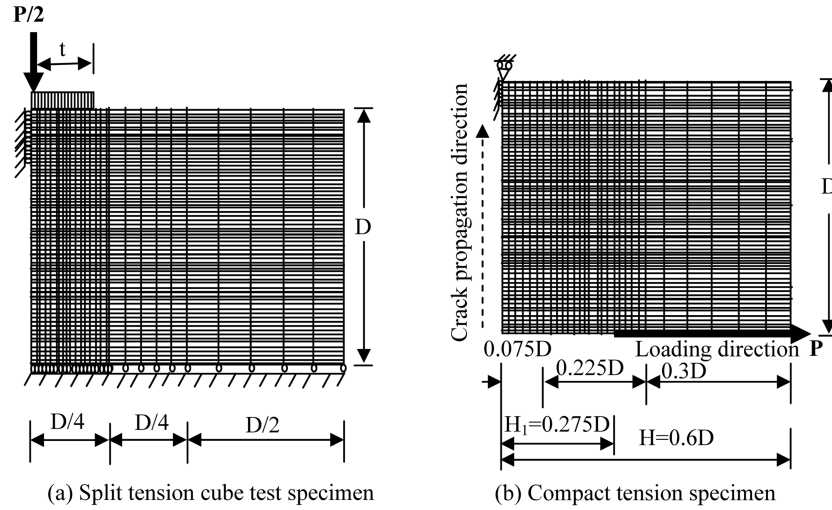


Fig. 5 Finite element discretization of test geometries

$D = 200-500$ mm, the finite element analysis is carried out for which the one-quarter of STC and half of CT specimens are discretized due to symmetry as shown in Fig. 5 considering 80 numbers of equal isoparametric plane elements along the characteristic dimension D . In the discretization, both the specimens are divided into three bands perpendicular to characteristic dimension D such as $D/4$, $D/4$ and $D/2$ in case of STC specimen and $0.075D$, $0.225D$ and $0.3D$ in case of CT specimen as shown in Fig. 5. This arrangement will facilitate to obtain finer mesh size near the potential fracture line. For STC specimen, the number of divisions is taken as 20, 5 and 5 in the bands $D/4$, $D/4$ and D respectively whereas it is 6, 18 and 6 in the bands $0.075D$, $0.225D$ and $0.3D$ respectively for CT specimen. Ten nodes from top along the potential fracture line are restrained against horizontal movement and all the nodes at the bottom perpendicular to fracture line are restrained against vertical movement in case of STC specimen. Three nodes from top and the topmost node along the potential fracture line are restrained in horizontal and vertical directions respectively in case of CT specimen. The concrete mix with material properties: $\nu = 0.18$, $f_i = 3.21$

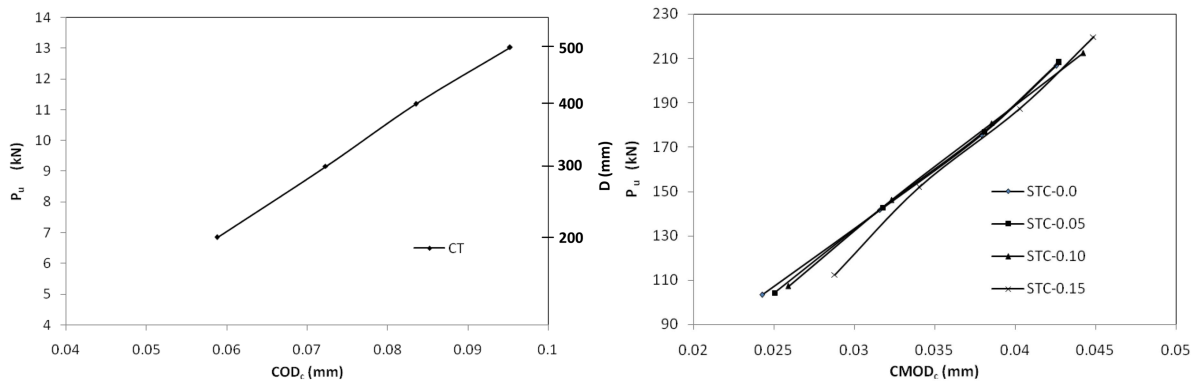


Fig. 6 P_u - COD_c curve for CT specimen at a_o/D ratio of 0.3
 Fig. 7 P_u - $CMOD_c$ curve for split-tension cube test at a_o/D ratio of 0.3

Table 2 Relative values of P_u and $CMOD_c$ for STC specimens for different specimen sizes

D (mm)	a_o/D	$\frac{P_{u,STC}}{P_{u,CT}}$				$\frac{CMOD_{c,STC}}{COD_{c,CT}}$			
		Value of β for STC				Value of β for STC			
		0.0	0.05	0.1	0.15	0.0	0.05	0.1	0.15
500	0.3	15.867	15.9787	16.309	16.867	0.447	0.4487	0.464	0.471
400	0.3	15.7017	15.81974	16.163	16.744	0.4547	0.456	0.461	0.483
300	0.3	15.4607	15.5867	15.954	16.584	0.437	0.439	0.447	0.471
200	0.3	15.0817	15.227	15.660	16.405	0.4127	0.426	0.440	0.490

Note: (i) $P_{u,STC}$ and $P_{u,CT}$ are the peak loads obtained for STC and CT specimens respectively.

(ii) $CMOD_{c,STC}$ and $COD_{c,CT}$ are the crack opening displacements at peak loads obtained for STC and CT specimens respectively.

MPa, $E = 30$ GPa, and $G_F = 103$ N/m along with nonlinear stress-displacement softening relation with $c_1 = 3$ and $c_2 = 7$ are used as the input parameters of FCM.

The results of peak load P_u from simulation of FCM versus COD_c for CT specimen at a constant a_o/D ratio of 0.3 are plotted in Fig. 6. Similar results of peak load P_u is plotted with the corresponding $CMOD_c$ at different load distributed widths ($\beta = 0.0, 0.05, 0.1$ and 0.15) for STC specimens of varying sizes (200-500 mm) at a constant a_o/D ratio of 0.3 as shown in Fig. 7. The legends of Fig. 7 are denoted by the type of specimen geometry and the load distributed widths.

Since it is difficult to show the specimen size on Fig. 7, Table 2 is presented for further clarification of the results shown in Fig. 7. Table 2 illustrates the values of P_u and $CMOD_c$ for STC specimen with reference to those values of CT specimen at corresponding specimen size.

6. Results and discussion

6.1 Fracture parameters of split-tension cube specimen and comparison

A comprehensive computer program in MATLAB is developed for the complete mathematical calculation according to the methods described in the previous sections. The values of P_u - $CMOD_c$ for STC and P_u - COD_c for CT specimens obtained from FCM were used to determine double- K fracture parameters. The *weight function method* with four terms is applied to calculate double- K fracture parameters in which the value of critical crack extension a_c is obtained using Eq. (1) for STC specimen. In this case, first of all the four parameters M_1 , M_2 and M_3 of four terms weight function are computed using Eqs. (17)-(19) and then closed form expression (Eq. (20)) is used to obtain the value of K_{IC}^C and finally the K_{IC}^{ini} is determined using inverse procedure (Eq. (9)). The nonlinear softening function as mentioned in the previous section is used in *weight function method* to obtain the double- K fracture parameters. For CT specimen, double- K fracture parameters were determined in a similar manner using five terms weight function method as mentioned elsewhere (Kumar and Barai 2008a, 2009a). Thus the values of K_{IC}^{un} , K_{IC}^C and K_{IC}^{ini} as obtained for STC for different distributed-load widths ($0 \leq \beta \leq 0.15$) and CT specimens for specimen size $200 \leq D \leq 500$ mm at a_o/D ratio of 0.3 are plotted through Figs. 8, 9 and 10 respectively.

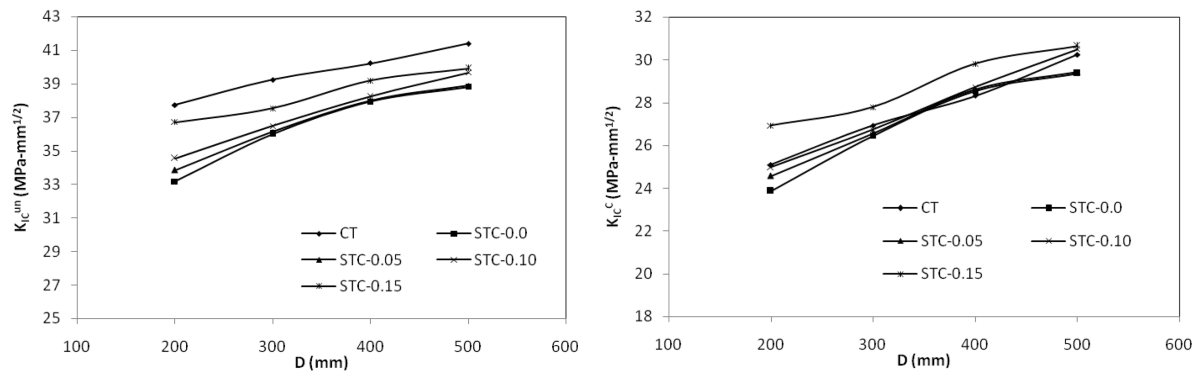


Fig. 8 Comparison of unstable fracture toughness between STC and CT tests Fig. 9 Comparison of cohesive toughness between STC and CT tests

From Fig. 8 it is seen that the unstable fracture toughness obtained from STC specimen is compatible with that of CT specimen. The value of K_{IC}^{un} for STC is the lowest for distributed-load width $\beta=0$ and is the highest for $\beta=0.15$ which is in close agreement with that obtained from CT specimen for all sizes of specimens. The values of K_{IC}^{un} are 36.70 and 39.91 MPa-mm^{1/2} for STC for $\beta=0.15$ and 37.72 and 41.40 MPa-mm^{1/2} for CT specimens for specimen size 200 and 500 mm respectively. That means the unstable fracture toughness of concrete can be determined using STC specimen with all advantages as mentioned in the previous sections.

The value of cohesive toughness for STC and CT specimens shown in Fig. 9 also shows that these values either obtained using STC specimen or CT specimen are in consistent with each other. For STC, the cohesive toughness values are slightly in higher side for $\beta=0.15$. That means STC specimen can predict almost the same results of cohesive toughness like other cracked specimen and hence it can be used with a great advantage similar to other commonly available fracture testing specimens.

From the results of initiation toughness for STC and CT specimens as shown in Fig. 10 it can be observed the this value for STC specimen has significant difference as compared with that obtained for CT specimen. The initial cracking toughness values for STC specimen are in lower side as compared with those of CT specimen for all values of distributed-load width ($0 \leq \beta \leq 0.15$)

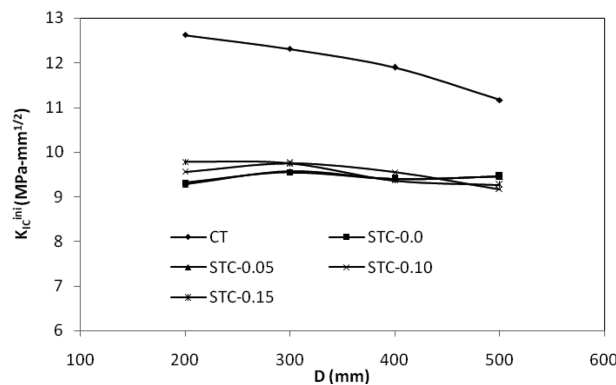


Fig. 10 Comparison of initial cracking toughness between STC and CT tests

considered in the study. On an average, these values for STC for all values of β ($0 \leq \beta \leq 0.15$) are less than those for CT specimen by approximately 23% and 16% for $D = 200$ mm and $D = 500$ mm respectively. It can be further seen from the figure that the values of K_{IC}^{ini} for STC specimen are not significantly influenced by specimen size whereas those values are influenced by specimen size in case of CT specimen. However, further experimental and numerical study needs to be carried out to conclude such generalized behavior. From this study it is clear the double- K fracture parameters can be determined from STC tests with a greater ease as compared with those obtained using other commonly available test specimens such as three-point bend test, compact tension specimen, wedge-splitting test and four-point bending specimen geometries. The results of these fracture parameters using STC specimens are consistent and comparable with those calculated using other tests geometries. A comprehensive experimental and numerical study on the double- K fracture parameters using split-tension cube test should be carried out in the future to investigate the behavior of these parameters considering wide range of material properties and geometrical parameters.

6.2 Effect of distributed-load width on the fracture parameters obtained using STC specimen

An additional parameter that is the distributed-load width does affect the results of fracture parameters obtained using split-tension cube test unlike TPBT, CT and WST specimens. This effect can be observed from Figs. 8-10 in which the fracture parameters as obtained using STC specimen are shown for varying values of β ranging 0-0.15 for the specimen size ranging 200-500 mm at a_0/D ratio of 0.3. The values of K_{IC}^{um} for $\beta=0$ are 33.18 and 38.82 MPa-mm^{1/2} for $D = 200$ and 500 mm respectively where as for $\beta=0.15$ those values are 36.71 and 39.91 MPa-mm^{1/2} for $D = 200$ and 500 mm respectively. Similarly, the values of K_{IC}^C for $\beta=0$ are 23.87 and 29.36 MPa-mm^{1/2} for $D = 200$ and 500 mm respectively where as those values for $\beta=0.15$ are 26.93 and 30.65 MPa-mm^{1/2} for $D = 200$ and 500 mm respectively. Hence, the values of K_{IC}^{ini} for $\beta=0$ are 9.32 and 9.46 MPa-mm^{1/2} for $D = 200$ and 500 mm respectively where as those values for $\beta=0.15$ are 9.78 and 9.26 MPa-mm^{1/2} for $D = 200$ and 500 mm respectively. It can be observed from the results of fracture parameters that there is an increase in the values of K_{IC}^{um} and K_{IC}^C for increasing values of distributed-load widths where as the effect of distributed-load width is almost insignificant on the value of K_{IC}^{ini} . If compared between the $\beta=0$ and 0.15, there is an increase in the K_{IC}^{um} of 9.62 and 2.73% for $D = 200$ and 500 mm respectively where as this increase for the K_{IC}^C is 11.36 and 4.20% for specimen size 200 and 500 mm respectively.

7. Conclusions

In the present work formulation for determination of double- K fracture parameters using weight function method for split-tension cube test was presented and the results of the initial cracking toughness, cohesive toughness and unstable fracture toughness were compared with those obtained using standard compact tension specimen. The advantage of lightness and compactness and simplicity in carrying out the fracture test using split-tension cube specimen can be exploited over the other standard cracked test specimens. Further, the developed weight function method can avoid the application of skilled numerical technique caused because of singularity problem at integral boundary occurring when determining the fracture parameters and thus they can be determined even using calculator. From the present study it can be concluded that the double- K fracture parameters

as obtained using split-tension cube test are in good agreement and consistent with those as calculated using standard compact tension specimen. However, the results of fracture parameters are influenced by the distributed-load width during loading the specimen in the split-tension cube test and it was observed that the values of unstable fracture toughness and cohesive toughness increase with increase in the distributed-load width where as the initial cracking toughness is not significantly affected by the distributed-load width. Finally it can be concluded that more numerical and experimental studies should be carried out in the future for recommending the split-tension cube specimen for its use in the standard fracture tests.

References

- ASTM International Standard E399-06 (2006), "Standard test method for linear-elastic method plane-strain fracture toughness K_{IC} of metallic materials", Copyright ASTM International, West Conshohocken, U.S., 1-32.
- Bažant, Z.P. and Oh, B.H. (1983), "Crack band theory for fracture of concrete", *Mater. Struct.*, **16**(93), 155-177.
- Bažant, Z.P., Kazemi, M.T., Hasegawa, T. and Mazars, J. (1991), "Size effect in Brazilian split-cylinder tests: measurements and fracture analysis", *ACI Mater. J.*, **88**(3), 325-332.
- Bažant, Z.P., Kim, J.K. and Pfeiffer, P.A. (1986), "Determination of fracture properties from size effect tests", *J. Struct. Eng. - ASCE*, **112**(2), 289-307.
- Brühwiler, E. and Wittmann, F.H. (1990), "The wedge splitting test: a method of performing stable fracture mechanics tests", *Eng. Fract. Mech.*, **35**, 117-125.
- Bueckner, H.F. (1970), "A novel principle for the computation of stress intensity factors", *Z. Angew. Math. Mech.*, **50**, 529-546.
- Carneiro, F.L. and Barcellos, A. (1949), "Re Âsistance a la Traction des Be Âtons", *Int. Assoc. Test Res. Lab. Mater. Struct. RILEM Bull.*, **13**, 98-125.
- Carpinteri, A. (1989), "Cusp catastrophe interpretation of fracture instability", *J. Mech. Phys. Solid.*, **37**(5), 567-582.
- Glinka, G. and Shen, G. (1991), "Universal features of weight functions for cracks in Mode I", *Eng. Fract. Mech.*, **40**, 1135-1146.
- Hillerborg, A., Modeer, M. and Petersson, P.E. (1976), "Analysis of crack formation and crack growth in concrete by means of fracture mechanics and finite elements", *Cement Concrete Res.*, **6**, 773-782.
- Ince, R. (2010), "Determination of concrete fracture parameters based on two-parameter and size effect models using split-tension cubes", *Eng. Fract. Mech.*, **77**, 2233-2250.
- Ince, R. and Arici, E. (2004), "Size effect in bearing strength of concrete cubes", *Constr. Build. Mater.*, **18**, 603-609.
- Jenq, Y.S. and Shah, S.P. (1985), "Two parameter fracture model for concrete", *J. Eng. Mech. - ASCE*, **111**(10), 1227-1241.
- Kadleček, V. Sr., Modry, S. and Kadleček, V. Jr. (2002), "Size effect of test specimens on tensile splitting strength of concrete: general relation", *Mater. Struct.*, **35**, 28-34.
- Karihaloo, B.L. (1986), "Fracture toughness of plain concrete from compression splitting tests", *Int. J. Cement Compos. Lightweight Concrete*, **8**(4), 251-259.
- Karihaloo, B.L. and Nallathambi, P. (1991), "Notched beam test: Mode I fracture toughness. Fracture Mechanics test methods for concrete", Report of RILEM Technical Committee 89-FMT (Edited by S.P. Shah and A. Carpinteri), Chamman & Hall, London, 1-86.
- Kumar, S. and Barai, S.V. (2008a), "Influence of specimen geometry on determination of double- K fracture parameters of concrete: a comparative study", *Int. J. Fracture*, **149**, 47-66.
- Kumar, S. and Barai, S.V. (2008b), "Cohesive crack model for the study of nonlinear fracture behaviour of concrete", *J. Inst. Eng. (India)*, **CV 89**, 7-15.
- Kumar, S. and Barai, S.V. (2009a), "Determining double- K fracture parameters of concrete for compact tension and wedge splitting tests using weight function", *Eng. Fract. Mech.*, **76**, 935-948.

- Kumar, S. and Barai, S.V. (2009b), "Effect of softening function on the cohesive crack fracture parameters of concrete CT specimen", *Sadhana-Acad. P. Eng. S.*, **36**(6), 987-1015.
- Kumar, S. and Barai, S.V. (2010), "Determining the double-K fracture parameters for three-point bending notched concrete beams using weight function", *Fatigue Fract. Eng. Mater. Struct.*, **33**(10), 645-660.
- Kumar, S. (2010), "Behaviour of fracture parameters for crack propagation in concrete", Ph.D. Thesis submitted to Indian Institute of Technology, Kharagpur, India.
- MATLAB, Version 7, The MathWorks, Inc. Copyright, 1984-2004.
- Nallathambi, P. and Karihaloo, B.L. (1986), "Determination of specimen-size independent fracture toughness of plain concrete", *Mag. Concrete Res.*, **38**(135), 67-76.
- Nilsson, S. (1961), "The tensile strength of concrete determined by splitting tests on cubes", *RILEM Bull.*, **11**(6), 63-67.
- Petersson, P.E. (1981), "Crack growth and development of fracture zone in plain concrete and similar materials", Report No. TVBM-100, Lund Institute of Technology.
- Planas, J. and Elices, M. (1991), "Nonlinear fracture of cohesive material", *Int. J. Fracture*, **51**, 139-157.
- Reinhardt, H.W., Cornelissen, H.A.W. and Hordijk, D.A. (1986), "Tensile tests and failure analysis of concrete", *J. Struct. Eng. - ASCE*, **112**(11), 2462-2477.
- Rice, J.R. (1972), "Some remarks on elastic crack-tip stress fields", *Int. J. Solids Struct.*, **8**, 751-758.
- RILEM Draft Recommendation (TC50-FMC) (1985), "Determination of fracture energy of mortar and concrete by means of three-point bend test on notched beams", *Mater. Struct.*, **18**(4), 287-290.
- Rocco, C., Guinea, G.V., Planas, J. and Elices, M. (1999), "Size effect and boundary conditions in the Brazilian test: theoretical analysis", *Mater. Struct.*, **32**, 437-444.
- Tada, H., Paris, P.C. and Irwin, G.R. (2000), *Stress analysis of cracks handbook*, 3rd Ed. New York, ASME Press.
- Tang, T., Bažant, Z.P., Yang, S. and Zollinger, D. (1996), "Variable-notch one-size test method for fracture energy and process zone length", *Eng. Fract. Mech.*, **55**, 383-404.
- Timoshenko, S.P. and Goodier, J.N. (1970), *Theory of elasticity*, 3rd Ed. New York: McGraw Hill.
- Tschegg, E.K. (1986), "Equipment and appropriate specimen shapes for tests to measure fracture values", Patent application (AT 390328), Austria.
- Wittmann, F.H., Rokugo, K., Bruhwiler, E., Mihashi, H. and Simopnin, P. (1988), "Fracture energy and strain softening of concrete as determined by compact tension specimens", *Mater. Struct.*, **21**(1), 21-32.
- Wu, Z., Jakubczak, H., Glinka, G., Molski, K. and Nilsson, L. (2003), "Determination of stress intensity factors for cracks in complex stress fields", *Arch. Mech. Eng.*, **L**(1), s41-s67.
- Xu, S. and Reinhardt, H.W. (1998), "Crack extension resistance and fracture properties of quasi-brittle materials like concrete based on the complete process of fracture", *Int. J. Fracture*, **92**, 71-99.
- Xu, S. and Reinhardt, H.W. (1999a), "Determination of double-K criterion for crack propagation in quasi-brittle materials, Part I: Experimental investigation of crack propagation", *Int. J. Fracture*, **98**, 111-149.
- Xu, S. and Reinhardt, H.W. (1999b), "Determination of double-K criterion for crack propagation in quasi-brittle materials, Part II: Analytical evaluating and practical measuring methods for three-point bending notched beams", *Int. J. Fracture*, **98**, 151-177.
- Xu, S. and Reinhardt, H.W. (1999c), "Determination of double-K criterion for crack propagation in quasi-brittle materials, Part III: Compact tension specimens and wedge splitting specimens", *Int. J. Fract.*, **98**, 179-193.
- Xu, S. and Reinhardt, H.W. (2000), "A simplified method for determining double-K fracture parameters for three-point bending tests", *Int. J. Fracture*, **104**, 181-209.
- Xu, S. and Zhang, X. (2008), "Determination of fracture parameters for crack propagation in concrete using an energy approach", *Eng. Fract. Mech.*, **75**, 4292-4308.
- Yang, S., Tang, T., Zollinger, D.G. and Gurjar, A. (1997), "Splitting tension tests to determine concrete fracture parameters by peak-load method", *Adv. Cement Based Mater.*, **5**, 18-28.

Abbreviations

CBM	crack band model
CMOD	crack mouth opening displacement
CMOD _c	critical value of crack mouth opening displacement
COD	crack opening displacement
COD _c	critical value of crack opening displacement
CT	compact tension
CTOD	crack-tip opening displacement
CTOD _c	critical value of crack-tip opening displacement
DGFM	double- <i>G</i> fracture model
DKFM	double- <i>K</i> fracture model
ECM	effective crack model
FCM	fictitious crack model
FPBT	four-point bending test
FPZ	fracture process zone
LEFM	linear elastic fracture mechanics
SEM	size effect model
SIF	stress intensity factor
STC	split-tension cube
TPBT	three-point bending test
TPFM	two parameter fracture model
WST	wedge splitting test.